RSC Advances

This is an *Accepted Manuscript*, which has been through the Royal Society of Chemistry peer review process and has been accepted for publication.

Accepted Manuscripts are published online shortly after acceptance, before technical editing, formatting and proof reading. Using this free service, authors can make their results available to the community, in citable form, before we publish the edited article. This *Accepted Manuscript* will be replaced by the edited, formatted and paginated article as soon as this is available.

You can find more information about *Accepted Manuscripts* in the Information for Authors.

Please note that technical editing may introduce minor changes to the text and/or graphics, which may alter content. The journal's standard Terms & Conditions and the Ethical guidelines still apply. In no event shall the Royal Society of Chemistry be held responsible for any errors or omissions in this *Accepted Manuscript* or any consequences arising from the use of any information it contains.

ROYAL SOCIETY OF CHEMISTRY

www.rsc.org/advances

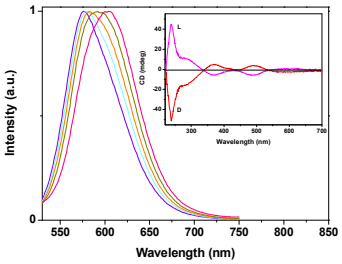

Ag_2S-Zn NCs exhibited tunable PL emission at 500 to 700 nm and clear mirror-image relationship in their CD signals.

RSC Advances Accepted Manuscript

Synthesis and characterization of chiral Ag_2S and Ag_2S-Zn nanocrystals

Ying-Fan Liu[1,2]*, Lei Wang[1], Wan-Zhen Shi[1],Yan-Hui Zhang[1],

Shao-Ming Fang[1,2]*

[1]Henan Provincial Key Laboratory of Surface and Interface Science,

[2]Henan Collaborative Innovation Center of Environmental Pollution Control and Ecological Resoration, Zhengzhou University of Light Industry, No. 166, Science Avenue, Zhengzhou 450001, China.

* Corresponding authors. Tel.: +86 0371 86609676; fax: +86 0371 86609676.

E-mail addresses: yfliu@zzuli.edu.cn (Y.-F. Liu), mingfang@zzuli.edu.cn (S.-M. Fang).

Abstract This paper focuses on the synthesis of novel chiral Ag_2S and Ag_2S-Zn nanocrystals (NCs) with chiral Pen as capping reagent in aqueous solution. Luminescence studies indicated the prepared Ag_2S and Ag_2S-Zn NCs all exhibited size-tunable photoluminescence (PL) emission at 500 to 700 nm. Compared with Ag_2S, the PL emission of the Ag_2S-Zn NCs could improve by around 2.4-fold. XRD results indicated the XRD patterns of the as-prepared Ag_2S NCs were weak, whereas the XRD of the Ag_2S-Zn NCs had the characteristics of a monoclinic crystal structure. Circular dichroism (CD) test showed that the prepared NCs exhibited a clear mirror-image relationship in their CD signals at 300 to 700 nm and Zn^{2+} played a key role of Cotton effect for the NCs. The chiral and fluorescent properties

RSC Advances Accepted Manuscript

of these NCs are likely to find widespread applications in bioimaging, chemical and biosensing, and possibly in asymmetry catalysis.

Keywords: chirality; luminescence; Ag_2S; Ag_2S-Zn; nanocrystals

Introduction

In the last two decades, the development of semiconductor nanocrystals (NCs）with multifunction such as using as fluorescence probes in cell imaging and biological labeling, chiral detection etc., has attracted much attention. [1-3] Compared with organic dyes, semiconductor NCs present a series of excellent optical properties, including size-dependent tunable photoluminescence, broad excitation spectrum, narrow emission bandwidth and high photochemical stability. [4-6] Unfortunately, most of the highly luminescent NCs are cytotoxic due to containing toxic heavy metals elements (Cd, Hg, Pb, etc.). [7-9] Ag_2S is an I_2−VI semiconductor with a direct band gap of 1.1 eV, and does not contain highly toxic heavy metals. [10-12] This material might be a promising candidate for fluorescence probes. Although various routes have been reported for the synthesis of Ag_2S NCs, they involved preparations at high temperature and dispersions in organic solvents, both of which made the nanocrystals inapplicable to biological system. [13-16] Generally, with water-soluble thiols as transferring reagents, the hydrophobic quantum dots can be transferred to hydrophilic semiconductor nanoparticles. [17] Hong et al reported that the Ag_2S NCs were firstly synthesized in an organic phase, the hydrophobic Ag_2S NCs were then coated with a surfactant dihydrolipoic acid (DHLA) and reacted with amine-functionalized PEG, using ethyl(dimethylaminopropyl) carbodiimide /N-hydroxysuccinimide (EDC/NHS) to afford highly water soluble Ag_2S NCs. [18] Nevertheless, aqueous synthesis of Ag_2S NCs is less reported. [19] This can be partly attributed to the fact that water-soluble Ag_2S clusters show a strong tendency to aggregate into

RSC Advances Accepted Manuscript

bulk, which complicates their synthesis considerably. As compared with the organic one, [20-22] aqueous synthesis of NCs is more reproducible, cheaper, and less toxic. The hydrophilicity of the products holds a great promise in biological application. Recently, aqueous synthesis allows formation of near-IR emitting Ag_2S NCs using 2-mercaptopropionic acid as a coating. [23] However, apart from near-IR luminescence, other optical properties, such as vis-luminescence and chirality etc, have not been reported. Therefore, it is a great challenge to synthesize water-soluble Ag_2S NCs with multifunction.

Very recently, much attention is paid on elucidating chirality in NCs owing to the widespread use of chirally modified nanoclusters surfaces for enantioselective catalysis and chiral analysis applications. [24-27] Surface in situ functionalization by chiral molecules is an effective strategy for chirality on nanoclusters. According to this strategy, we have reported the synthesis and chiroptical properties of optically active silver nanoclusters protected by a pair of enantiomers of chiral penicillamine. [28] Chiral NCs have been scarcely synthesized and studied in the literature. One example is D- or L-penicillamine-capped NCs. [29] However, the origin of chirality or optical activity in NCs has not been fully understood. Here with d-penicillamine (d-Pen) and l-penicillamine (l-Pen) as the capping reagent, we present a novel method of synthesis of chiral Ag_2S and Ag_2S-Zn NCs in aqueous solutions. In our experiments, we found that Zn^{2+} ions played a key role for the chirality of the NCs.

Experimental Section

Chemicals: d-penicillamine (99%, d-Pen), l-penicillamine (99%, l-Pen) and $NaBH_4$ (96%) were obtained from Sigma, Inc. Thioacetamide (TAA) and $AgNO_3$ were obtained from Shanghai Chemical Reagents Company. Highpurity deionized water (>18.3 MΩ/cm) was produced by Millipore A10 Milli-Q.

RSC Advances Accepted Manuscript

Synthesis of Pen capped-Ag_2S NCs: All the solutions were freshly prepared with deionized water prior to the synthesis. The Ag_2S NCs could be prepared by the simple one-pot process by using silver nitrate as a precursor, NaOH as a basic catalyst and TAA as a sulfide source at 60℃. In a typical synthesis, 74.6 mg (0.5 mmol) of Pen was dissolved in the solution containing 95 mL of water and 0.9 mL of 0.5 M NaOH. After stirring at 60℃ for 30 min, 2.5 mL of 0.1M silver nitrate aqueous solution and 1.2 mL of 0.1 M TAA solution were added, respectively. The resulting mixture solution between Ag^+ and TAA was heated to 60℃ under open-air conditions and refluxed at different time for controlling the size of NCs. Aliquots of the reaction solution were removed at regular intervals for UV absorption and PL experiments.

Synthesis of Pen capped-Ag_2S-Zn NCs: A typical synthesis of Ag_2S-Zn NCs is described hereafter. The 100 mL of as-prepared Pen-capped Ag_2S solution was heated to 60 ℃ under open-air conditions, and then 1.2 mL of 0.1 M $ZnAc_2$ and 0.6 mL of 0.1 M TAA were added. The solution was heated to 60℃ at different time for controlling the sizes of NCs. Aliquots of the reaction solution were removed at regular intervals for UV absorption and PL experiments.

Characterization. UV–vis absorption and photoluminescence (PL) spectra were measured at room temperature with a Shimadzu UV-3100 spectrophotometer and a Hitachi 7000 fluorescence spectrometer, respectively. PL spectra were taken at the excitation wavelength λex = 400 nm. Time-resolved luminescence measurements were carried out on a Fluorolog-3 spectroflurometer with LED lamp as light source. Ludox was applied for PL lifetime measurement in order to eliminate the influence of light scattering (i.e., excitation and emission). Circular dichroism (CD) spectra were measured at Applied Photophysics Ltd chirasan spectrophotometer. The concentrations of Ag_2S and Ag_2S-Zn NCs were set same and diluted to the original solution 10%, and the NCs were purified with a

RSC Advances Accepted Manuscript

10 kDa dialysis membrane for CD characterization. For all structural characterization, Ag_2S (A) and Ag_2S-Zn (B) samples were obtained after heating 31 and 14 min, respectively. Powder XRD measurements were taken on a Philips X'Pert PRO X-ray diffractometer. High-resolution transmission electron microscopy (HRTEM) was performed on a Philips FEI Tecnai G^2 20 S-TWIN.

3. Results and discussion

XRD, TEM and XPS characterization

Powder X-ray diffractions (XRD) were carried out on the as-formed products. The XRD of the Ag_2S NCs powder sample (Fig. 1A) exhibits a broad and intense (121) peak of silver at 2θ = ~35°. For Ag_2S-Zn NCs, all of the peaks in the XRD patterns (Fig. 1B) matched those of monoclinic α-Ag_2S (JCPDS 14-0072). The characteristic monoclinic planes of 111, 112, 121, 220 and 213 locating at 25.79°, 29.18°, 31.66°, 34.94°, 36.78°, 43.47°, and 53.29° have been observed. Compared with the XRD patterns of the Ag_2S and Ag_2S-Zn samples, the XRD patterns of the as-prepared Ag_2S NCs were undistinguishable, whereas the XRD of the Ag_2S-Zn NCs had the characteristics of a monoclinic crystal structure, the results showed that the prepared Ag_2S-Zn NCs had perhaps better PL emission than that of Ag_2S NCs. It was noted that the XRD intensity for the Ag_2S-Zn NCs was found to be similar to the Ag_2S QDs, which perhaps was due to excess ligands attaching to the surfaces of the Ag_2S-Zn NCs.

Generally, the size and size distribution are critically important for luminescent NCs. The TEM images in Fig. 2A and B demonstrate that the Ag_2S and Ag_2S-Zn NCs are well-dispersed and have a near-spherical shape. The average diameters of the Ag_2S and Ag_2S -Zn NCs are 4.5+0.1 and 5.0+0.2 nm, respectively. We further carried out energy dispersive X-ray spectroscopy (EDX) measurements

RSC Advances Accepted Manuscript

for Pen-capped Ag_2S (A) and Ag_2S-Zn (B) NCs. The EDX spectra show the existence of Ag and S in the Ag_2S (A) and Ag_2S-Zn (B) samples (Fig. 3). Compared with Ag_2S, the Zn peak at 1.01 keV in the new sample occurs evidently, indicating the formation of Ag_2S-Zn nanoparticles. The N peaks at 0.27 KeV are from the stabilizer Pen.

In order to confirm the formation of Ag_2S-Zn NCs in aqueous solution, X-ray photoelectron spectroscopy (XPS) measurements were made. A full survey scan and Ag, Zn, S photoelectron spectra of the Ag_2S-Zn are displayed in Fig. 4. Besides the Ag levels, the spectra are dominated by the C1s and O1s signals stemming from the capping agent. XPS spectra in Fig. 4 show that there exist Ag3d, Zn2p and S2p. The two peaks in Fig. 4B of 1021.9 eV and 1045.1 eV can be assigned to the binding energy of Zn 2p3/2 and Zn 2p1/2, respectively, which corresponds to Zn^{2+} according to the previous results. [30–32] The peaks with binding energies of 367.8 eV and 373.8 eV correspond to Ag 3d5/2 and Ag 3d3/2, respectively, which is characteristic of Ag^+ in the Ag_2S product in Fig. 4C [33]. The peak at 161.3 eV belongs to S2p1/2 in a zinc–sulfur bond and silver–sulfur bond in composites. [33] These data of X-ray photoelectron spectroscopy (XPS) provide the direct evidence of the formation of Ag_2S-Zn NCs.

The optical properties of Ag_2S NCs

Aqueous Ag_2S NCs could be easily synthesized using Pen as stabilizer at 60℃. Fig. 5 presents typical evolutions of both absorption and PL spectra of Pen-stabilized Ag_2S NCs prepared in aqueous solution. Before heating, there was a UV–vis absorption peak at 501 nm ascribe to un-passivated Ag_2S NCs, because the extremely low solubility of the Ag_2S ($K_{SP} = 6.3\times10^{-50}$) results in fast crystal growth, even though at the presence of Pen. However, no fluorescence was observed with this crude solution. Under heating at 60℃, these colloid clusters started to crystallize and the fluorescence of the solution

RSC Advances Accepted Manuscript

appeared. As shown in Fig. 5(A), during heating from 0 to 15 min, the absorptivity was significantly increased and the absorption band-edge red-shifted, which indicated that the sizes of Ag_2S NCs gradually increased. At longer reaction time from 15 to 79 min, the absorption onset had not apparent change and significant absorptivities increasing were observed. As shown in Fig. 5(B), after heating 15 min, the as-synthesized Ag_2S NCs exhibit orange luminescence with an emission peak around 577 nm. For heating time of 18, 26, 31, and 79 min, Ag_2S NCs are obtained with maximum PL emission at 584, 588, 596, and 610 nm, respectively (Fig. 5B). When heating for 31 min, the PL intensity reaches a plateau. By further heating, the PL intensity started to decrease. The red-shift of the PL is accord with the absorption band-edge, perhaps due to the increase of the NCs. [34]

The optical properties of Ag_2S-Zn NCs

Fig. 6 presents typical evolutions of both absorption and PL spectra of Pen-stabilized Ag_2S and Ag_2S-Zn NCs prepared in aqueous solution. Absorption spectra of Ag_2S-Zn NC fractions taken after 15, 18, 26, 31 and 79 min of heating at 60℃ are compared with the spectra of Ag_2S NCs. In comparison with the Ag_2S NCs, the absorption maximum of the first electronic transition as-prepared Ag_2S-Zn NCs evidently shifts-blue in wavelength, which perhaps is attributed to that addition of a ZnS shell could confine the Ag_2S NCs wavefunction. The absorption in Ag_2S-Zn NCs shifts to longer wavelengths as the particles grow in the course of heating, which is typical characteristic of core-shell NCs. [35-37] Emission spectra of Ag_2S-Zn NCs heated for different times are shown in Fig. 6B in comparison to Ag_2S reference sample. As shown in Fig. 6(B), after heating for 3 min, the PL emission of the as-synthesized Ag_2S-Zn NCs also arises blue-shift with an emission peak around 575 nm, which is similar to the absorption spectrum. Further heating for 6, 14, 24, 39, 54, and 84 min, Ag_2S-Zn NCs are obtained with maximum PL emission at 577, 578, 579, 584, 592, and 603 nm, respectively. After

RSC Advances Accepted Manuscript

heating for 14 min, the PL intensity reaches a plateau and the maximum emission of the NCs increase by around 2.4-fold. The observed PL enhancement is caused by passivation of surface trap states due to formation of core-shell NCs and then the PL decrease as a function of heating time is perhaps due to formation of new surface trap along with thicker ZnS shell. [38]

According to relevant documents, [39, 40] red NCs with <700 nm PL emission are generally very small (< 2.6 nm in diameter). For examples, Pang's group successfully synthesized octylamine-capped Ag_2S NCs (690 nm) with sizes of 1.5 nm. [39] Gui et al reported that using multidentate polymers (poly(acrylic acid)-graft- cysteamine- graftethylenediamine) as stabilizer, aqueous Ag_2S NCs with 2.6 nm sizes were prepared, displaying 687 nm PL. [40] More works on Ag_2S NCs have shown that QD diameters of 4-5 nm generally display NIR PL spectra (>700 nm). [39-41] In this paper, we reported that using small molecules thiol (Pen) as stabilizer, Ag_2S and Ag_2S-Zn NCs with sizes ranging 4-5 nm display visible PL emission. The reason may be owing to that at the presence of Pen stabilizer, extremely small Ag_2S NCs (such as 1~2 nm) arise aggregation in aqueous solution and thus the observed visible PL is actually from extremely small NCs.

In order to reveal further the intrinsic reason for the unique evolution of PL spectrum, PL relaxations of NCs were characterized. The obtained PL decay curves of the Ag_2S and Ag_2S-Zn NCs are shown in Fig.7. In general, these PL decay curves at a peak wavelength of 600 nm (λ_{ex} =390 nm) can be well fitted by a biexponential equation $I(t)=A_1Exp(-t/\tau_1) + A_2Exp(-t/\tau_2)$ [42-44]. The constants obtained by the fitting are tabulated in Table1. The observed lifetime were 3.14$\pm$0.12 ns (74.87%) and 27.10$\pm$0.32 ns (25.13%) for Ag_2S NCs, whereas 3.47$\pm$0.11ns and 33.72$\pm$0.35 ns for Ag_2S-Zn NCs. The average lifetime of the Ag_2S and Ag_2S-Zn NCs were 9.16 ns and 10.92 ns, respectively. Obviously, the average emission lifetime of the latter was longer than that of the former. It is well-known that surface defect states are formed during

RSC Advances Accepted Manuscript

the surface modification of Ag_2S NCs with Pen, and they lead to the nonradiative decays of excitons. As for Ag_2S-Zn NCs, the excitons generated by excitation with wavelength 390 nm were created in the cores of Ag_2S and confined in the cores energetically lower than ZnS shells which effectively protected them from nonradiative decays. The reduction of the non-radiative decay rate was accompanying the increase of the radiative lifetime, resulting in improvement of the luminescence properties of the NCs. Therefore, compared with that of Ag_2S NCs, the longer average lifetime of Ag_2S-Zn NCs was attributed to the decrease of surface defect states and the increase of the radiative lifetime.

The chiroptical properties of the Ag_2S andAg_2S-Zn NCs

Fig.8. displays the absorption spectra of Ag_2S and Ag_2S-Zn samples and CD spectra of Pen, the complex of Pen and Ag^+, Ag_2S and Ag_2S-Zn NCs. The absorption spectra and the CD spectra were measured at same time with Applied Photophysics Ltd chirasan spectrophotometer. From Fig.8 A and Fig.8 B, it is evident that the absorption peak of D-Pen capped Ag_2S NCs coincides with that of L-Pen capped Ag_2S NCs, as expected, and the absorptivities of chiral Pen capped Ag_2S and Ag_2S-Zn NCs are almost same at 300 to 700 nm. The Pen provides opposite CD responses in the wavelength at 224 nm. With respect to pure Pen, the additional chiral features appear at 249, 278 and 322 nm for the mixture of Ag cations and chiral Pen (Fig.8D), which can be ascribed to formation of an Ag-Pen complex. Compared with Pen (Fig. 8C) and the mixture of (D, L)-Pen and Ag^+, which present prominent peaks at 224, 249, 278 and 322 nm, Ag_2S and Ag_2S-Zn NCs stabilized by chiral Pen show additional broad CD features between 322 and 700 nm (Fig. 8E and Fig. 8F). Thus, Pen molecules adsorbed on NC surfaces not only preserve their own chirality but also induce chirality on the Ag_2S and Ag_2S-Zn core. Compared with Ag_2S, it is evident that the Ag_2S-Zn NCs exhibit strong chiral peaks at 371, 492 and 594 nm, which shows that Zn^{2+} can greatly improve the CD features of the NCs. The origin of the

RSC Advances Accepted Manuscript

difference of chirality in the NCs between Ag_2S and Ag_2S-Zn is unclear at present, but some possibilities can be stated: (i) The interaction of the chiral ligand and NCs. The Ag_2S NCs tends to aggregate, whereas Ag_2S-Zn NCs not only have good stability, but also exhibit strong PL and CD features. Compared with Ag_2S NCs, the strong interaction between chiral-Pen ligand and Ag_2S-Zn NCs perhaps improves the stability of the NCs, resulting in strong CD signals. (ii) The difference in the electronic structure between Ag_2S andAg_2S-Zn might influence their deformability. Thus, passivation of NCs with chiral molecules results in unique electronic and chiroptical responses that are unlike those of the component parts. These optically active NCs exhibited Cotton effects or clear mirror-image relationship in their CD signals with the anisotropy factors increasing with the Zn^{2+} adding into the NCs.

The stability of the Ag_2S and Ag_2S-Zn NCs

It was noted that the as-prepared Ag_2S NCs exhibited photostability several days, whereas Ag_2S-Zn NCs have excellent colloidal and photostability over three months of study. In order to further study the stability of the NCs, we investigated them by the Zeta potential (ζ). Zeta potential was used to determine the surface charge densities of Ag_2S and Ag_2S-Zn NCs. Fig. 9 shows that the ζ of Ag_2S and Ag_2S-Zn solution reach 20.8 mV and 34.4 mV, respectively, indicating that the surface charge was dominated by the bound Pen. The ζ of the Ag_2S-Zn solution increases to 13.6 mV, resulting in increasing the repulsion of the different NCs, which is agreed with the stability of the NCs. The changes in ζ may be attributed to the different electronic interaction of NCs (positive charges) and Pen (negative charges). Therefore, using chiral Pen as stabilizer, we have synthesized not only highly luminescent NCs with strong chiral signals, but

RSC Advances Accepted Manuscript

also more stable NCs in aqueous solution.

Summary

In summary, to the best of our knowledge, this is the first report of a synthesis of chiral Ag_2S and Ag_2S-Zn NCs. The prepared Pen-stabilized NCs exhibited size-tunable PL emission at 500 to 700 nm. Compared with Ag_2S, the PL emission of the Ag_2S-Zn NCs could improve by around 2.4-fold. The prepared NCs exhibited a clear mirror-image relationship in their circular dichroism (CD) signals at 300 to 700 nm. It was unexpected that Zn^{2+} played a key role of Cotton effect for the NCs. The chiral and fluorescent properties of these NCs are likely to find widespread applications in bioimaging, chemical and biosensing, and possibly in asymmetry catalysis.

Acknowledgments

This work was financially supported by the Natural Science Foundation of China (Nos. 21171150 and 21271159) and Henan Province Science and Technology Programs (No. 112102210002).

References

[1] X. Michalet, F. F. Pinaud, L. A. Bentolila, J. M. Tsay, S. Doose, J. J. Li, G. Sundaresan, A. M. Wu, S. S. Gambhir and S. Weiss, *Science*, 2005, **307**, 538.

[2] S. Kim, Y. T. Lim, E. G. Soltesz, A. M. De Grand, J. Lee, A. Nakayama, J. A. Parker, T. Mihaljevic, R. G. Laurence, D. M. Dor, L. H. Cohn, M. G. Bawendi and J. V. Frangioni, *Nat. Biotechnol.*, 2004, **22**, 93.

[3] X. H. Gao, Y. Y. Cui, R. M. Levenson, L. W. K.Chung and S. M. Nie, *Nat. Biotechnol.*, 2004, **22**, 969.

[4] H. Peng, L. Zhang, T. H. M. Kjallman, C. Soeller and J. Travas-Sejdik, *J. Am. Chem. Soc.*, 2007, **129**, 3048.

RSC Advances Accepted Manuscript

[5] J. Ma, J. Y. Chen, Y. Zhang, P. N. Wang, J. Guo, W. L. Yang and C. C. Wang, *J. Phys. Chem. B*, 2007, **111**, 12012.

[6] Z. Deng, Y. Zhang, J. Yue, F. Tang and Q. Wei, *J. Phys. Chem. B*, 2007, **111**, 12024.

[7] N. Lewinski, V. Colvin and R. Drezek, *Small*, 2008, **4**, 26.

[8] L. D. Chen, J. Liu, X. F. Yu, M. He, X. F. Pei, Z. Y. Tang, Q. Q. Wang, D. W. Pang and Y. Li, *Biomaterials*, 2008, **29**, 4170.

[9] D. W. Deng, J. F. Xia, J. Cao, L. Z. Qu, J. M. Tian, Z. Y. Qian, Y. Q. Gu and Z. Z. Gu, *J. Colloid Interface Sci.*, 2012, **367**, 234.

[10] A.W.Tang, Y. Wang, H. H. Ye, C. Zhou, C. H. Yang, X. Li, H. S. Peng, F. J. Zhang, Y. B. Hou and F. Teng, *Nanotechnology*, 2013, **24**, 355602.

[11] B. Liu and Z. F. Ma, *Small*, 2011, **7**, 1587.

[12] L. Han, Y. Y. Lv, A. M. Asiri, A. O. Al-Youbi, B. Tu and D. Y. Zhao, *J. Mater. Chem.*, 2012, **22**, 7274.

[13] H. Liu, W. Hu, F. Ye, Y. Ding and J. Yang, *RSC Advances*, 2013, **3**, 616.

[14] Y. P. Du, B. Xu, T. Fu, M. Cai, F. Li, Y. Zhang and Q. B. Wang, *J. Am. Chem. Soc.*, 2010, **132**, 1470.

[15] P. Li, Q. Peng and Y. D. Li, *Chem.-Eur. J.*, 2011, **17**, 941.

[16] T. G. Schaaff and A. J. Rodinone, *J. Phys. Chem. B*, 2003, **107**, 10416.

[17] J. M. Klostranec and W. C. W. Chan, *Adv. Mater.*, 2006, **18**, 1953.

[18] G. Y. Hong, J. T. Robinson, Y. J. Zhang, S. Diao, A. L. Antaris, Q. B. Wang and H. J. Dai, *Angew. Chem.*, 2012, **124**, 9956.

[19] L. Dong, Y. Chu, Y. Liu and L. Li, *J. Colloid Interf. Sci.*, 2008, **317**, 485.

[20] M. Yarema, S. Pichler, M. Sytnyk, R. Seyrkammer, R. T. Lechner, G. Fritz-Popovski, D. Jarzab, K. Szendrei, R. Resel, O. Korovyanko, M. A. Loi, O. Paris, G. N. Hesser and W. Heiss, *ACS Nano*, 2011, **5**, 3758.

[21] P. Jiang, Z. Q. Tian, C. N. Zhu, Z. L. Zhang and D. W. Pang, *Chem. Mater.*, 2011, **24**, 3.

[22] A. Sahu, L. Qi, M. S. Kang, D. Deng and D. J. Norris, *J. Am. Chem. Soc.*, 2011, **133**, 6509.

[23] I. Hocaoglu, M. N. Cizmeciyan, R. Erdem, C. Ozen, A. Kurt, A. Sennaroglu and H. Y. Acar, *J. Mater. Chem.*, 2012, **22**, 14674.

[24] H. Yao, K. Miki, N. Nishida, A. Sasaki and K. Kimura, *J. Am. Chem. Soc.*, 2005, **127**, 15536.

RSC Advances Accepted Manuscript

[25] G. Shemer, O. Krichevski, G. Markovich, T. Molotsky, I. Lubitz and A. B. Kotlyar, *J. Am. Chem. Soc.*, 2006, **128**, 11006.

[26] C. Carrillo-Carrión, S. Cárdenas, B. M. Simonet and M. Valcárcel, *Anal. Chem.*, 2009, **81**, 4730.

[27] N. Nishida, H. Yao and K. Kimura, *Langmuir*, 2008, **24**, 2759.

[28] Y. F. Liu, G. Q. Wang, J. B. Zhao, L. Jiang, S. M. Fang and Y. A. Sun, *Colloids and Surfaces A*, 2013, **426**, 12.

[29] M. P. Moloney, Y. K. Gun'ko and J. M. Kelly, *Chem. Commun.*, 2007, **38**, 3900.

[30] M. Muruganandham, R. Amutha, E. Repo, M. Sillanpää, Y. Kusumoto and Md. Abdulla-Al-Mamun, *J. Photoch. Photobio. A*, 2010, **216**, 133.

[31] D. Q. Gao, G. J. Yang, J. Zhang, Z. H. Zhu, M. S. Si and D. S. Xue, *Applied Physics Letters*, 2011, **99**, 052502.

[32] Q. R. Zhao, Y. Xie, Z. G. Zhang and X. Bai, *Cryst. Growth Des.*, 2007, **7**, 153.

[33] S. G. Pan, X. H. Liu and X. Wang, *Materials Characterization*, 2011, **62**, 1094.

[34] R. D. Robinson, B. Sadtler, D. O. Demchenko, C. K. Erdonmez, L. W. Wang and A. P. Alivisatos, *Science*, 2007, **317**, 355.

[35] H. Bao, Y. Gong, Z. Li and M. Gao, *Chem. Mater.*, 2004, **16**, 3853.

[36] Y. He, H.-T. Lu, L.-M. Sai, W.-Y. Lai, Q.-L. Fan, L.-H. Wang and W. Huang, *J. Phys. Chem. B.*, 2006, **110**, 13370.

[37] Y. F. Liu, B. Xie, Z. G. Yin, S. M Fang and J. B. Zhao, *Eur. J. Inorg. Chem.*, 2010, **10**, 3010.

[38] Y. F. Liu and J. S. Yu, *J. Colloid Interf. Sci.*, 2010, **351**, 1.

[39] P. Jiang, Z.-Q. Tian, C.-N. Zhu, Z.-L. Zhang and D.-W. Pang, *Chem. Mater.*, 2012, **24**, 3.

[40] R. J. Gui, A. j. Wan, X. F. Liu, W. Yuan and H. Jin, *Nanoscale*, 2014, **6**, 5467.

[41] Y. J. Zhang, Y. S. Liu, C. Y. Li, X. Y. Chen and Q. B. Wang, *J. Phys. Chem. C*, 2014, **118**, 4918.

[42] D. E. Nam, W. S. Song and H. Yang, *J. Mater. Chem.*, 2011, **21**, 18220.

[43] X. Y. Wang, L. H. Qu, J. Y. Zhang, X. G Peng and M. Xiao, *Nano Lett.*, 2003, **3**, 1103.

[44] A. L. Rogach, T. Franzl, T. A. Klar, J. Feldmann, N. Gaponik, V. Lesnyak, A. Shavel, A. Eychmuller, Y. P. Rakovich and J. F. Donegan, *J. Phys. Chem. C*, 2007, **111**, 14628.

RSC Advances Accepted Manuscript

Figures and Captions

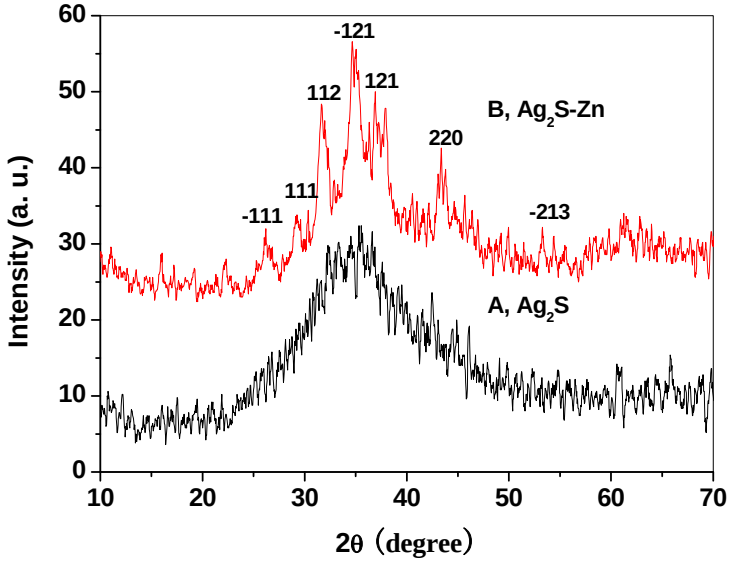

Fig. 1. XRD patterns of Ag_2S and Ag_2S-Zn NCs.

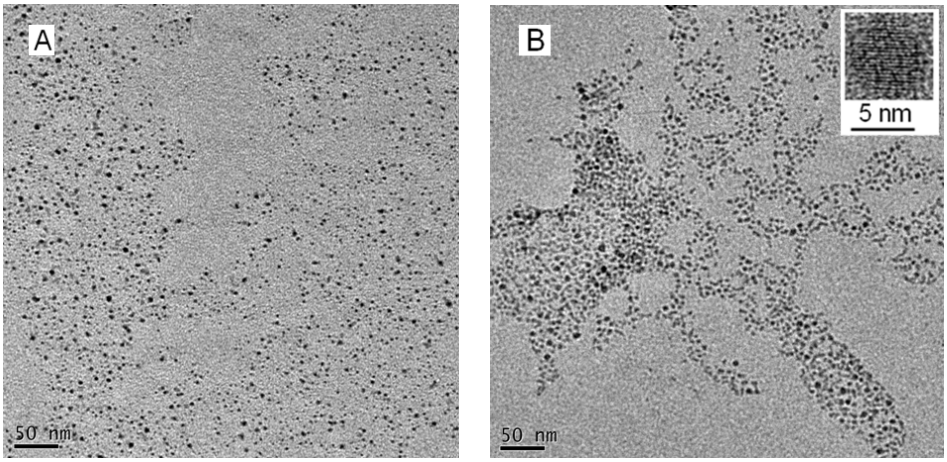

Fig. 2 TEM images of the Ag_2S (A) and Ag_2S-Zn (B) NCs. Inset: HR-TEM image of the Ag_2S-Zn NCs

RSC Advances Accepted Manuscript

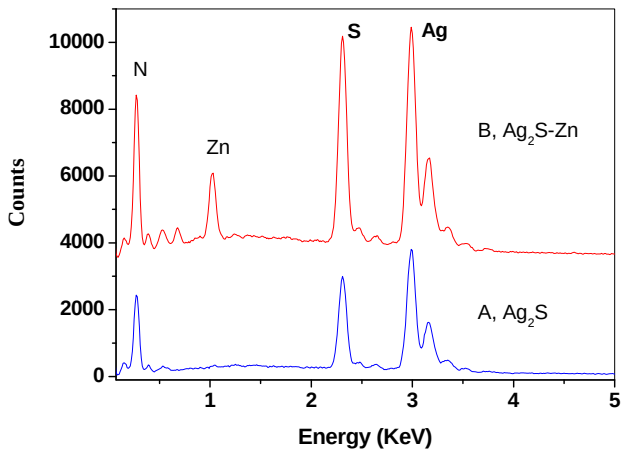

Fig. 3. Typical EDX spectra of Pen-capped Ag_2S (A) and Ag_2S-Zn (B) NCs.

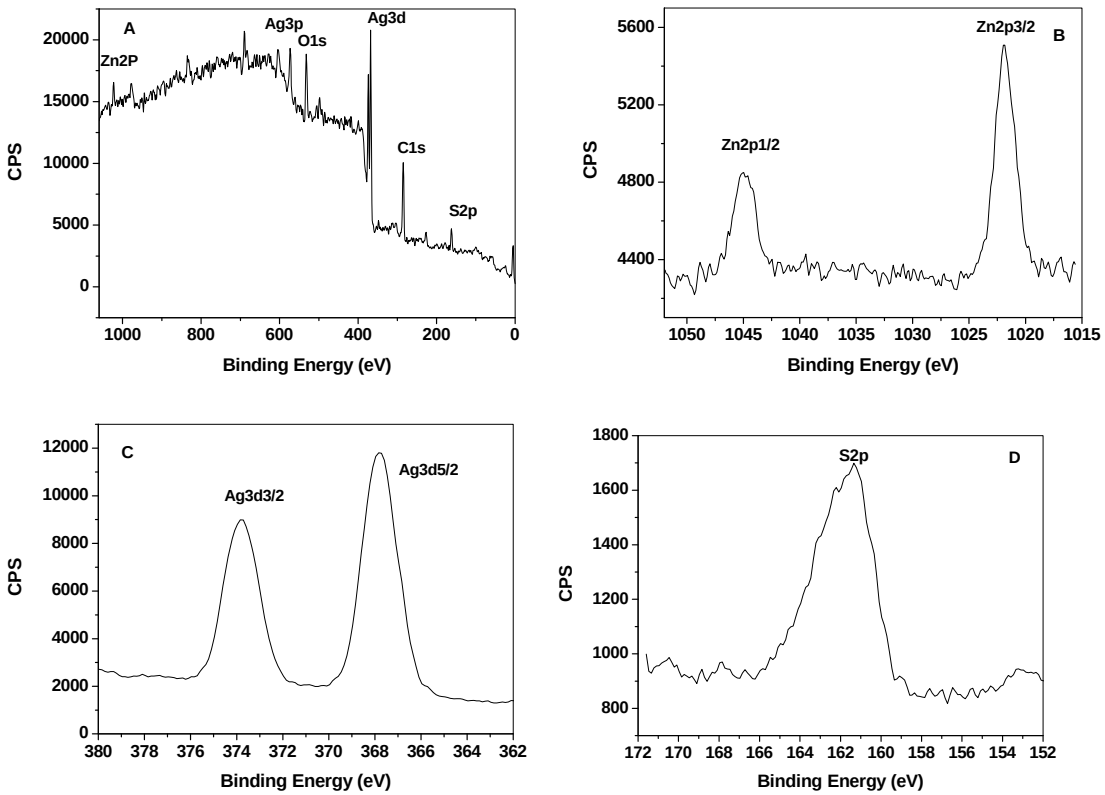

Fig. 4. The XPS spectra of (A) the whole survey, (B) Zn2p, (C) Ag3d, and (D) S2p of the as-prepared Ag_2S-Zn NCs.

RSC Advances Accepted Manuscript

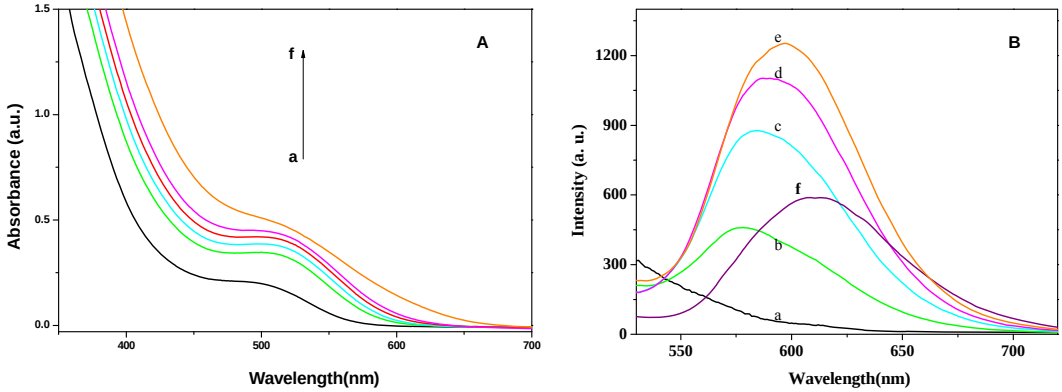

Fig. 5. Typical temporal evolution of the absorption (A) and corresponding emission (B) spectra of Ag_2S NCs. Curves **a** ~ **f** represent the absorption (A) and corresponding emission (B) spectra of Ag_2S NCs obtained for heating 0, 15, 18, 26, 31, and 79 min, respectively. The excitation wavelength was 400 nm.

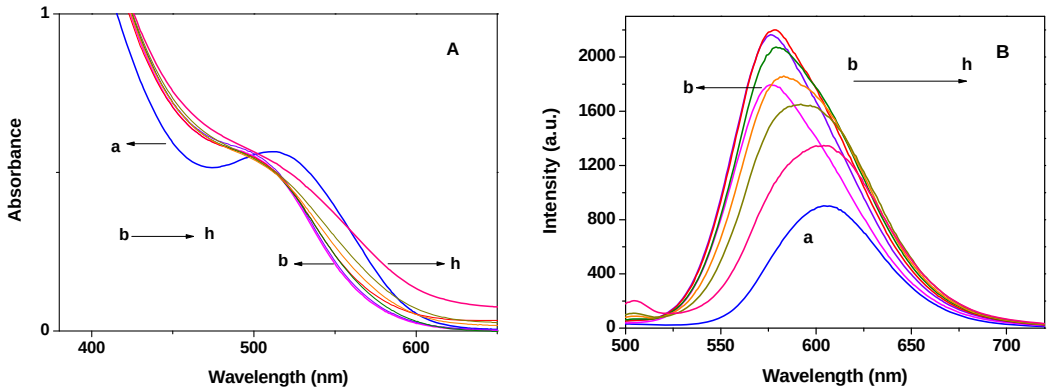

Fig. 6. Typical temporal evolution of the absorption (A) and corresponding emission (B) spectra of Ag_2S and Ag_2S-Zn NCs. Curve **a** represents the absorption (A) and corresponding emission (B) spectra of Ag_2S NCs. Curves **b** ~ **h** represent the absorption (A) and corresponding emission (B) spectra of Ag_2S-Zn NCs obtained for heating 3, 6, 14, 24, 39, 54 and 84 min, respectively. The excitation wavelength was 400 nm.

RSC Advances Accepted Manuscript

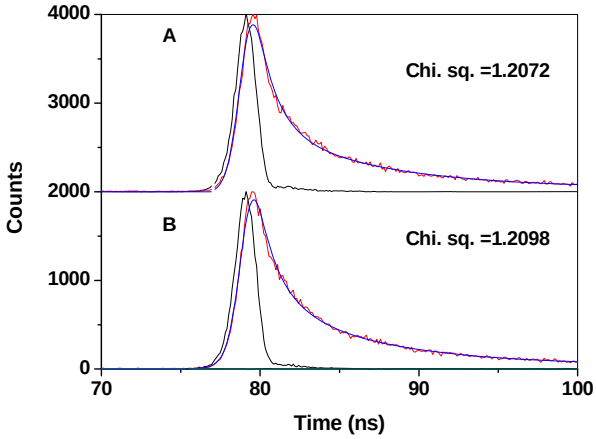

Fig. 7. PL time evolution spectra of the Ag_2S (A) and Ag_2S-Zn (B) samples. Ag_2S (A) and Ag_2S-Zn (B) NCs were obtained after heating 31 and 14 min, respectively. The excitation and emission wavelengths were 390 and 600 nm, respectively.

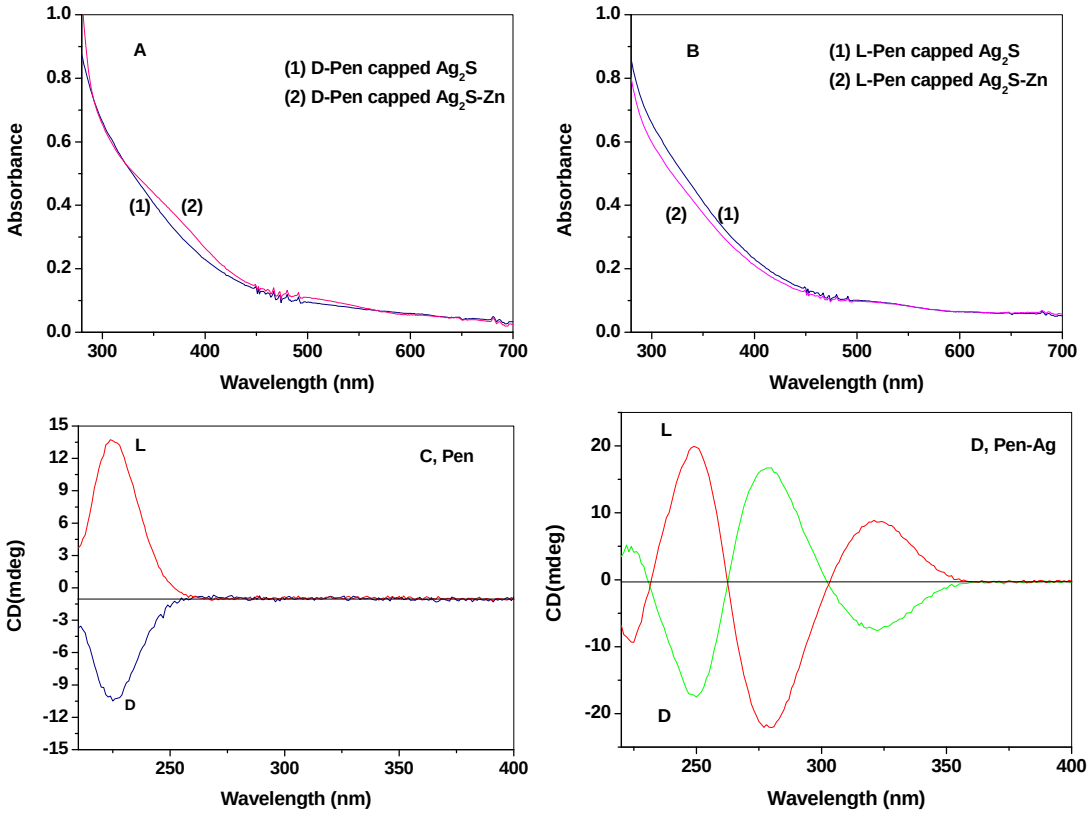

RSC Advances Accepted Manuscript

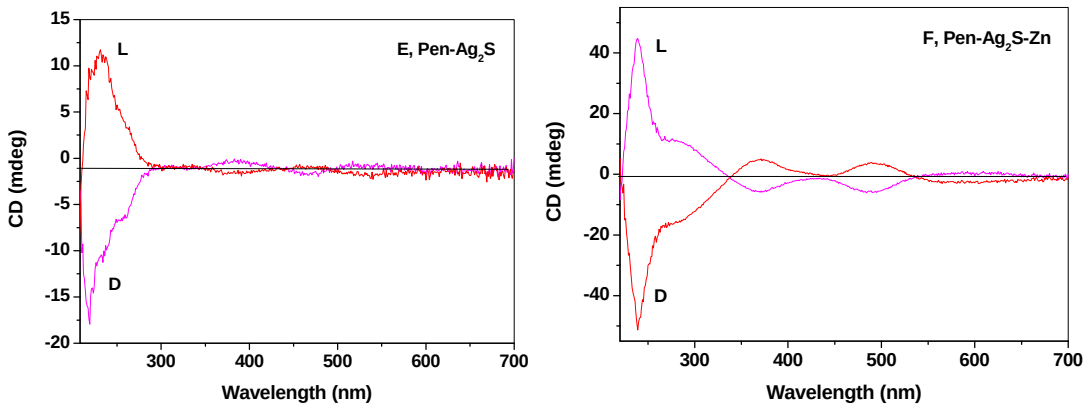

Fig. 8. Absorption spectra of D-Pen capped (A) and L-Pen capped (B) Ag_2S and Ag_2S-Zn samples. Circular dichroism spectra of Pen (C), the complex of Pen and Ag^+ (D), chiral Ag_2S (E) and Ag_2S-Zn NCs (F).

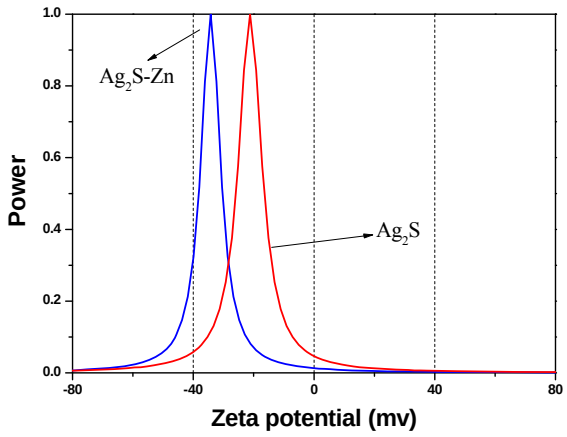

Fig.9. Zeta-potential measurements of Pen-capped Ag_2S and ZnS-Ag_2S NCs in aqueous solution.

Table

Table1 PL decay constants obtained from $I(t)=A_1Exp(-t/\tau_1) + A_2Exp(-t/\tau_2)$.

sample	τ_1/ns	A_1/%	τ_2/ns	A_2/%
Ag_2S	3.14±0.12	74.87	27.10±0.32	25.13
Ag_2S-Zn	3.47±0.11	74.76	33.72±0.35	25.24

RSC Advances Accepted Manuscript